



# Application of Palladium-Mediated $^{18}\text{F}$ -Fluorination to PET Radiotracer Development: Overcoming Hurdles to Translation

## Citation

Kamlet, Adam S., Constanze N. Neumann, Eunsung Lee, Stephen M. Carlin, Christian K. Moseley, Nickeisha Stephenson, Jacob M. Hooker, and Tobias Ritter. 2013. Application of palladium-mediated  $^{18}\text{f}$ -fluorination to pet radiotracer development: overcoming hurdles to translation. PLoS ONE 8(3): e59187.

## Published Version

doi:10.1371/journal.pone.0059187

## Permanent link

<http://nrs.harvard.edu/urn-3:HUL.InstRepos:11800764>

## Terms of Use

This article was downloaded from Harvard University's DASH repository, and is made available under the terms and conditions applicable to Other Posted Material, as set forth at <http://nrs.harvard.edu/urn-3:HUL.InstRepos:dash.current.terms-of-use#LAA>

## Share Your Story

The Harvard community has made this article openly available.  
Please share how this access benefits you. [Submit a story](#).

[Accessibility](#)

# Application of Palladium-Mediated $^{18}\text{F}$ -Fluorination to PET Radiotracer Development: Overcoming Hurdles to Translation

Adam S. Kamlet<sup>1</sup>, Constanze N. Neumann<sup>1</sup>, Eunsung Lee<sup>1</sup>, Stephen M. Carlin<sup>2</sup>, Christian K. Moseley<sup>2</sup>, Nickeisha Stephenson<sup>1</sup>, Jacob M. Hooker<sup>2,3\*</sup>, Tobias Ritter<sup>1,3\*</sup>

**1** Department of Chemistry and Chemical Biology, Harvard University, Cambridge, Massachusetts, United States of America, **2** Athinoula A. Martinos Center for Biomedical Imaging, Massachusetts General Hospital and Harvard Medical School, Charlestown, Massachusetts, United States of America, **3** Division of Nuclear Medicine and Molecular Imaging, Department of Radiology, Massachusetts General Hospital, Boston, Massachusetts, United States of America

## Abstract

New chemistry methods for the synthesis of radiolabeled small molecules have the potential to impact clinical positron emission tomography (PET) imaging, if they can be successfully translated. However, progression of modern reactions from the stage of synthetic chemistry development to the preparation of radiotracer doses ready for use in human PET imaging is challenging and rare. Here we describe the process of and the successful translation of a modern palladium-mediated fluorination reaction to non-human primate (NHP) baboon PET imaging—an important milestone on the path to human PET imaging. The method, which transforms  $^{18}\text{F}$ fluoride into an electrophilic fluorination reagent, provides access to aryl- $^{18}\text{F}$  bonds that would be challenging to synthesize via conventional radiochemistry methods.

**Citation:** Kamlet AS, Neumann CN, Lee E, Carlin SM, Moseley CK, et al. (2013) Application of Palladium-Mediated  $^{18}\text{F}$ -Fluorination to PET Radiotracer Development: Overcoming Hurdles to Translation. PLoS ONE 8(3): e59187. doi:10.1371/journal.pone.0059187

**Editor:** Gayle E. Woloschak, Northwestern University, United States of America

**Received:** November 28, 2012; **Accepted:** February 12, 2013; **Published:** March 12, 2013

**Copyright:** © 2013 Kamlet et al. This is an open-access article distributed under the terms of the Creative Commons Attribution License, which permits unrestricted use, distribution, and reproduction in any medium, provided the original author and source are credited.

**Funding:** This work was supported by the National Institutes of Health (NIH) (GM088237, MH093874, EB013042, S10RR017208, and S10RR022976). The funders had no role in study design, data collection and analysis, decision to publish, or preparation of the manuscript.

**Competing Interests:** The “System for Fluorination Organic Compounds” technology has been licensed in part by SciFluor Life Sciences. TR has financial interest in SciFluor. There are no further patents, products in development or marketed products relevant to this manuscript to declare. This does not alter the authors’ adherence to all the PLOS ONE policies on sharing data and materials.

\* E-mail: hooker@nmr.mgh.harvard.edu (JMH); ritter@chemistry.harvard.edu (TR)

## Introduction

Positron emission tomography (PET) is a non-invasive imaging technique used to characterize and diagnose disease [1,2]. Historically, PET imaging has been limited by chemistry. There are few convenient and efficient methods to incorporate positron-emitting isotopes into small molecules of imaging interest. Several positron-emitting isotopes are used for PET imaging, including carbon-11, nitrogen-13, oxygen-15, and copper-64, but due to its suitable half-life for synthesis and imaging, fluorine-18 ( $^{18}\text{F}$ ) is the most common and most relevant isotope for clinical PET [3,4]. Additionally, fluorine is present in a variety of biologically active molecules and pharmaceuticals [5,6]. However, synthesis with  $^{18}\text{F}$  is difficult due to time restrictions (half-life of  $^{18}\text{F}$ : 110 min) and mass restrictions (scale of synthesis: nanomoles), among others [7]. Thus the general chemical challenges associated with carbon-fluorine bond formation [8,9,10] are exacerbated for  $^{18}\text{F}$ -radiotracer synthesis. Modern methods for the construction of carbon-fluorine bonds are changing the landscape of molecules considered viable for PET [9]. The new chemical methods hold the unrealized potential of changing radiotracer design and development. A critical, non-trivial step is the development of modern fluorination methods from the stage of synthetic chemistry to the preparation of radiotracer doses ready for *in vivo* PET imaging. Here we describe the first successful development of a modern palladium-mediated fluorination reaction to be used for

non-human primate (NHP) PET imaging—an important milestone on the path to human PET imaging.

The imaging candidates reported here were chosen for structural motifs that are representative of drug-like small molecules, and were intended to highlight the utility of transition-metal-mediated carbon-fluorine bond formation to overcome chemical challenges associated with  $^{18}\text{F}$  chemistry. The challenges include: 1)  $^{18}\text{F}$  radiochemistry requires fast reaction rates because the concentration of the limiting reagent (fluoride) is small ( $\mu\text{M}$ ) compared to typical synthetic reactions ( $\text{mM}$  to  $\text{M}$ ). Slow reaction rates are often overcome by elevating reaction temperatures, which can lead to side reactions and product decomposition, especially for complex small molecules. 2)  $^{18}\text{F}$  is available in nucleophilic and electrophilic forms, but only the nucleophilic form,  $^{18}\text{F}$ fluoride, is readily available and can be made in high specific activity [7,11]. Specific activity is a measurement of the amount of radioactivity per molar amount of sample. High specific activity, though not necessary for all PET applications, is important for imaging biological targets of low concentration, like imaging of neurotransmitter receptors in the brain [4]. For pharmacokinetic measurements, specific activity is less critical. 3)  $^{18}\text{F}$ fluoride is created by the proton bombardment of  $^{18}\text{O}$  $\text{H}_2\text{O}$ . While removal of the bulk water is common for synthesis with  $^{18}\text{F}$ , the large hydration energy [12,13,14] and the small amount of fluoride prevents rigorous drying. Hydrated fluoride is less nucleophilic than dry fluoride and therefore cannot



with picoline provided complex **6** that can capture fluoride. Complex **6**, which can be synthesized on multi-gram scale, is not unique in its ability to capture fluoride. For example the pyridine (instead of picoline) analog of **6** can capture fluoride as well (see Supporting Information S1). Nevertheless, **6** is currently the complex of choice because the picoline ligand imparts enough electron-donating character to the electron-deficient palladium center for long-term storage, but can quickly be displaced by fluoride.

### Important Characteristics of High-valent Organometallic Complexes **6** and **7**

Complex **6** can capture <sup>18</sup>F from samples of [<sup>18</sup>F]fluoride (Figure 3, Step 1) and then serve as an electrophilic <sup>18</sup>F fluorination reagent (Figure 3, Step 2). Complex [<sup>18</sup>F]-**7** can be used as the electrophilic reagent, for the fluorination of pyridylsulfonamide-stabilized palladium (II) complexes **9** (see Figure 4) [30], and can provide access to electron-rich, electron-neutral, and electron-poor functionalized aryl fluorides. High-valent palladium complex **7** is likely the first of a class of complexes that exhibit the desired reactivity (capture and electrophilic transfer of fluoride to make C–F bonds).

The ability of **6** and **7** to capture and transfer fluoride is unusual. Complex **7** functions as an electrophilic reagent, similar to conventional electrophilic fluorination reagents previously used [30]. Yet, unequivocally, fluoride is the original source of fluorine. The generation of an electrophilic fluorination reagent from fluoride, without electrochemical methods, is challenging because fluorine is the strongest elemental oxidant known. From an electrostatic standpoint, the electropositive palladium center of

complex **6** is able to attract the fluoride anion. High-valent palladium(IV) fluoride **7** was designed to prevent unproductive C–F reductive elimination by the inclusion of multidentate ligands. Reductive elimination from octahedral complexes is typically preceded by ligand dissociation to a penta-coordinate species [29,31], which is disfavored by multidentate ligands. Additionally, tetrapyrazole borate ligands possess the ability to coordinate in either a bidentate or tridentate mode and can switch between them to accommodate the appropriate coordination chemistry needed. Specifically, tridentate coordination is important to stabilize the octahedral geometry for Pd(IV)d<sup>6</sup>, but, with minimal structural reorganization, bidentate coordination, of a square planar Pd(II)d<sup>8</sup> complex is possible, the geometry of the complex resulting after fluoride transfer. The ability to access different coordination modes may lower the activation barrier to fluorination. Finally the triflate counterion was chosen because it is non-coordinating so as to not displace fluoride from the palladium center, and it does not contain readily exchangeable fluoride. Common, non-coordinating counterions such as BF<sub>4</sub><sup>−</sup> and SbF<sub>6</sub><sup>−</sup> would introduce exogenous <sup>19</sup>F into the sample and lower the specific activity of the final molecule.

### Synthesis and Radiofluorination of Complex Small Molecules

Radiolabeled [<sup>18</sup>F]-**7** can be used as the electrophilic reagent in the palladium-mediated fluorination reaction we have previously disclosed [30] to form radiolabeled aryl fluorides (Figure 4). The mechanism of fluorination is proposed to occur by oxidation of and transfer of fluorine from [<sup>18</sup>F]-**7** to **9** to form a new Pd(IV)–<sup>18</sup>F complex, which can then undergo C–F reductive elimination to afford <sup>18</sup>F-labeled aryl fluoride. Evidence for oxidative fluorine transfer has been established: A high-valent aryl Pd(IV)–F complex could be observed by NMR spectroscopy after oxidation of an aryl Pd(II) complex, specifically **9** with the aryl and pyridine substituent linked, with **7** [24]. Complex small molecule substrates can be made in a modular fashion by transmetalation of aryl boronic acid derivatives with palladium acetate complex **8**, synthesized in four steps from commercially available reagents (see Supporting Information S1). Many palladium(II) aryl complexes, for example **15** and **20** (substrates leading to **1** and **2**), can be purified by chromatography on silica gel, are stable to air and moisture, and can be stored for extended periods of time without decomposition (>1 year). Syntheses of palladium aryl complexes **15** and **20** are shown in Figures 5 and 6.

Palladium complexes **15** and **20** were constructed from commercially available starting materials using a placeholder functional group at the eventual site of fluorination. For syntheses via late-stage fluorination of **1** and **2**, aryl bromides are used as the placeholders then changed to aryl boronic esters that can undergo transmetalation on to the palladium center in the penultimate step. There are no radiochemistry time constraints associated with the synthesis of the palladium aryl complexes, because <sup>18</sup>F is only incorporated after the palladium substrates are synthesized. For the non-chemists, fluorination precursors (e.g. **15**) are not trivial to make, but could be made available for purchase. Palladium complex **15**, the precursor to paroxetine (**1**) is synthesized via a route similar to a published route [32], but with an aryl bromide in lieu of an aryl fluoride, which simplifies access to the desired substrate. Alkylation, acylation, and cyclization reactions starting from 1-(4-bromophenyl)-3-chloropropan-1-one affords dihydropyridone **10** (Figure 5). Asymmetric conjugate reduction using conditions developed by Buchwald [32] provide enantioenriched δ-lactam **11** in 88% *ee*. Recrystallization of an intermediate later in the synthesis (**12**) provides material that is >99% *ee*. A Claisen

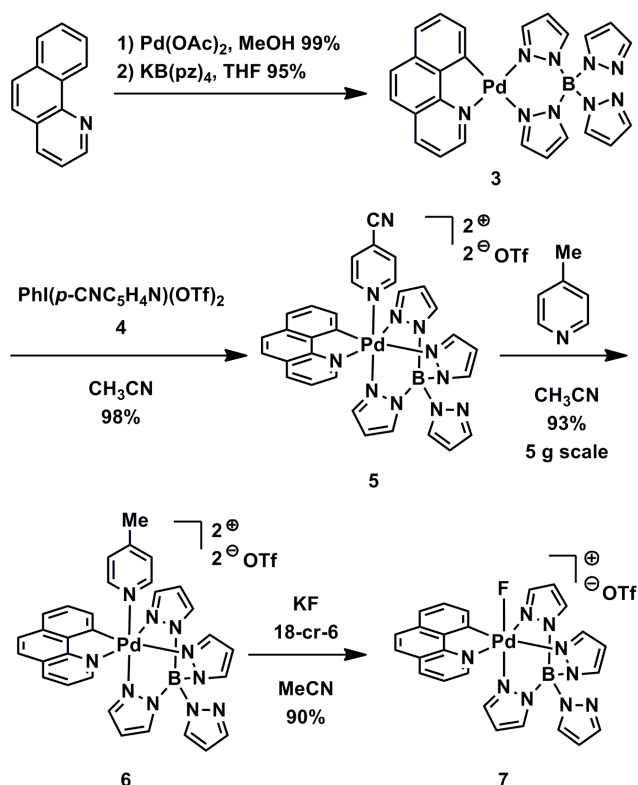


**Figure 2. New electrophilic fluorination reagent.** Synthesis of high-valent palladium complex **7** that is an electrophilic fluorination reagent derived from complex **6** through fluoride capture. doi:10.1371/journal.pone.0059187.g002

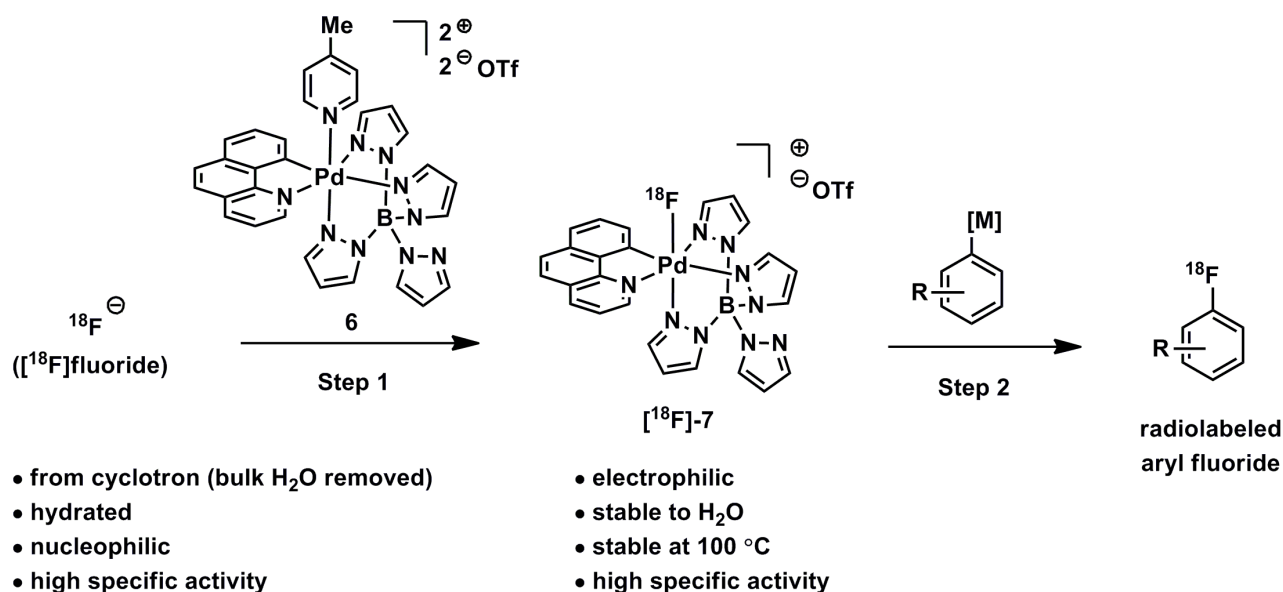


**Figure 3. Two-step procedure for synthesis of radiolabeled aryl fluorides.** The procedure consists of capture of [<sup>18</sup>F]fluoride by palladium(IV) complex **6** to form electrophilic [<sup>18</sup>F]-**7** and fluorine transfer to aryl metal complexes.

condensation followed by reduction gives alcohol **12**. Protecting group exchange followed by Mitsunobu reaction with sesamol and DIAD affords **13** that possesses the full carbon skeleton of paroxetine. Borylation yields **14** and transmetalation provides palladium complex **15**.

For the palladium complex **20** leading to 5-HT<sub>2C</sub> agonist **2**, alkylation, olefination, and reduction of 5-bromosalicylaldehyde affords allylic alcohol **16** that is used in a Charett asymmetric cyclopropanation reaction [33] to yield cyclopropane **17** in 96% *ee* (Figure 6). The enantiomeric excess can be upgraded at a later point (**18**) via recrystallization to >99% *ee*. Alcohol to amine conversion and deprotection leads to the aryl bromide **18** that undergoes palladium-catalyzed borylation to afford **19**. Aryl boronic ester is converted to palladium complex **20** through transmetalation.

We have found that the yield of the “cold” (<sup>19</sup>F) fluorination reactions for a given substrate roughly correlates with the radiochemical yield of the “hot” (<sup>18</sup>F) fluorination reactions. Palladium aryl substrates **15** and **20** were fluorinated with the non-radiolabeled (<sup>19</sup>F) version of palladium complex **6** to afford

small molecule aryl fluorides **21** and **22** in 71% and 72% yield, respectively (Figure 7; Equations 1 and 2). Removal of protecting groups reveals paroxetine (**1**) and the 5-HT<sub>2C</sub> agonist **2**.

### Scope and Limitations of Fluorination Reaction

Fluorination of **15** and **20** demonstrates the functional group tolerance of our protocol, and establishes that late-stage fluorination in the presence of a variety of functional group is possible for electron-rich arenes, that are often challenging to prepare with conventional fluorination reactions. Currently, our method does not tolerate nucleophilic, basic functional groups, such as certain amines. While pyridine-substituents are tolerated, amines of higher basicity such as tertiary alkyl amines are not. We have overcome this limitation in some cases through the use of protecting groups such as the Boc groups used for substrates **15** and **20**. Additionally, substitution besides hydrogen ortho to the site of fluorination reduces the efficiency of palladium aryl substrate synthesis and fluorination. An additional limitation is the required synthesis of the palladium complexes themselves. While generally stable, the synthesis requires some knowledge of organometallic chemistry.

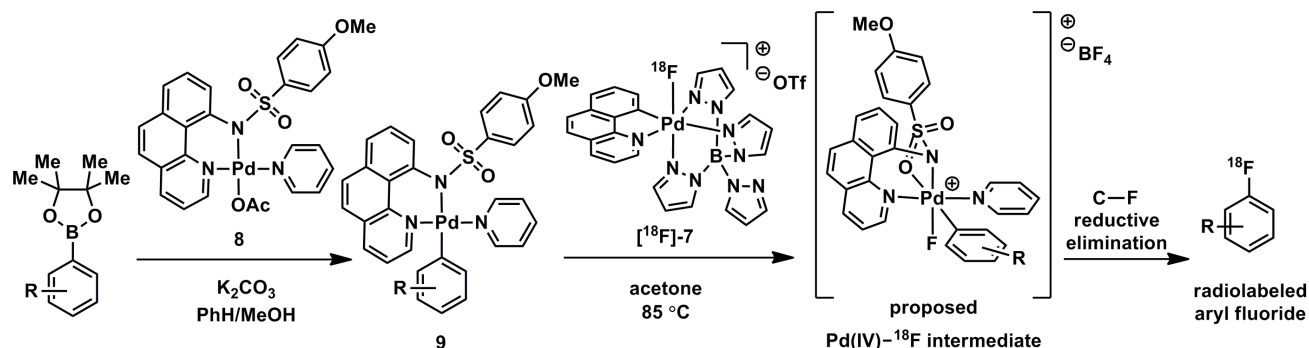


**Figure 4. General palladium-mediated synthesis of radiolabeled aryl fluorides.** C–F bond formation is proposed to occur by oxidation of **9** with [<sup>18</sup>F]-**7** leading to a proposed Pd(IV)–<sup>18</sup>F intermediate followed by C–F reductive elimination.

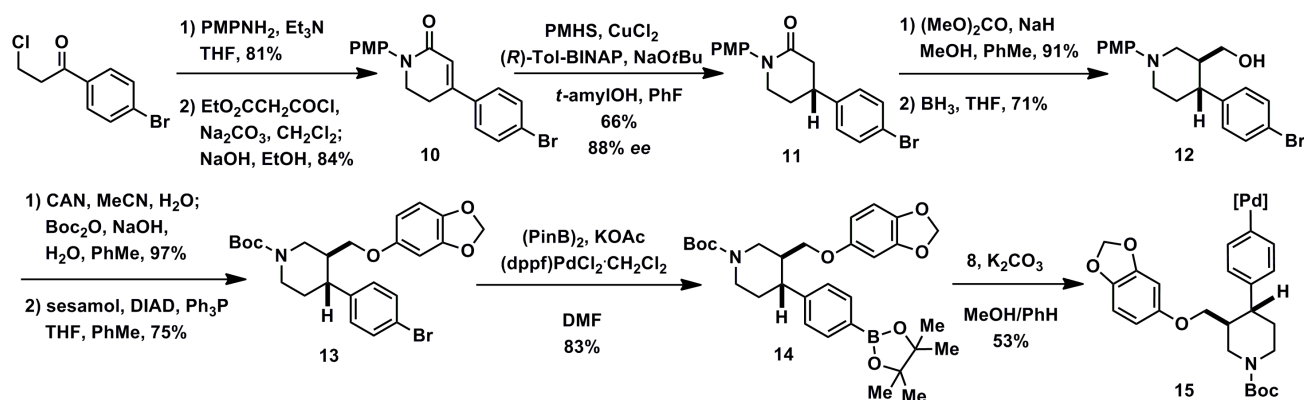


**Figure 5. Synthesis of palladium(II) aryl substrate 15.**

doi:10.1371/journal.pone.0059187.g005

### Practical and Procedural Considerations for the Transition to Radiochemistry

The syntheses of  $^{18}\text{F}$ -1 and  $^{18}\text{F}$ -2 with  $^{18}\text{F}$ fluoride were accomplished with procedural modifications based on the physical and practical differences between fluorination chemistry with  $^{18}\text{F}$  and  $^{19}\text{F}$ . First,  $^{18}\text{F}$ fluoride was prepared following common radiochemistry protocols from a sample produced in  $^{18}\text{O}$ H<sub>2</sub>O by a cyclotron [34]. Second, we adapted the procedures for the difference in stoichiometry between reactions with  $^{19}\text{F}$  and  $^{18}\text{F}$ . For high specific activity  $^{18}\text{F}$ fluoride reactions only nanomoles of the electrophilic fluorination reagent are synthesized, which remain in the presence of a large excess of **6**, the palladium precursor. In practice, we found that it was not feasible or advantageous to rapidly and cleanly isolate  $^{18}\text{F}$ -7 from the mixture. Therefore, the  $^{18}\text{F}$  method was modified into a two-step process with the reagent  $^{18}\text{F}$ -7 made *in situ*.

The two-step fluorination reaction can afford radiolabeled aryl fluorides on a scale suitable for PET imaging (Figure 8). Several variables were explored and optimized to accomplish efficient and

quick fluorination with  $^{18}\text{F}$ -7. Samples of  $^{18}\text{F}$ fluoride in H<sub>2</sub>O with KHCO<sub>3</sub> and the common phase transfer reagent, 18-crown-6, were azeotropically dried with MeCN and acetone (Figure 8A). 18-Crown-6 was chosen instead of common cryptand phase transfer reagents (e.g. Kryptofix® 2.2.2), because **5** reacts unproductively with the amine functionality found in Kryptofix® 2.2.2. Initial variability in terms of overall radiochemical yield was often associated with the drying process (“dry-down”) and resolubilizing of fluoride. While the reaction tolerates the presence of water, the efficiency decreases as water concentration increases. Next, palladium complex **5**, dissolved in acetone, was added for fluoride capture to form fluorinating reagent  $^{18}\text{F}$ -7 in less than 10 minutes. Before fluorination, the reaction mixture is filtered over a pyridine-functionalized resin, JandaJel™, as a quick intermediate purification step, which resulted in higher yields compared to experiments omitting filtration. Filtration removes byproducts that precipitate during the reaction. Pyridine-functionalized solid support is more effective than other filtration methods, which may be due to pyridine capturing **5** by displacing

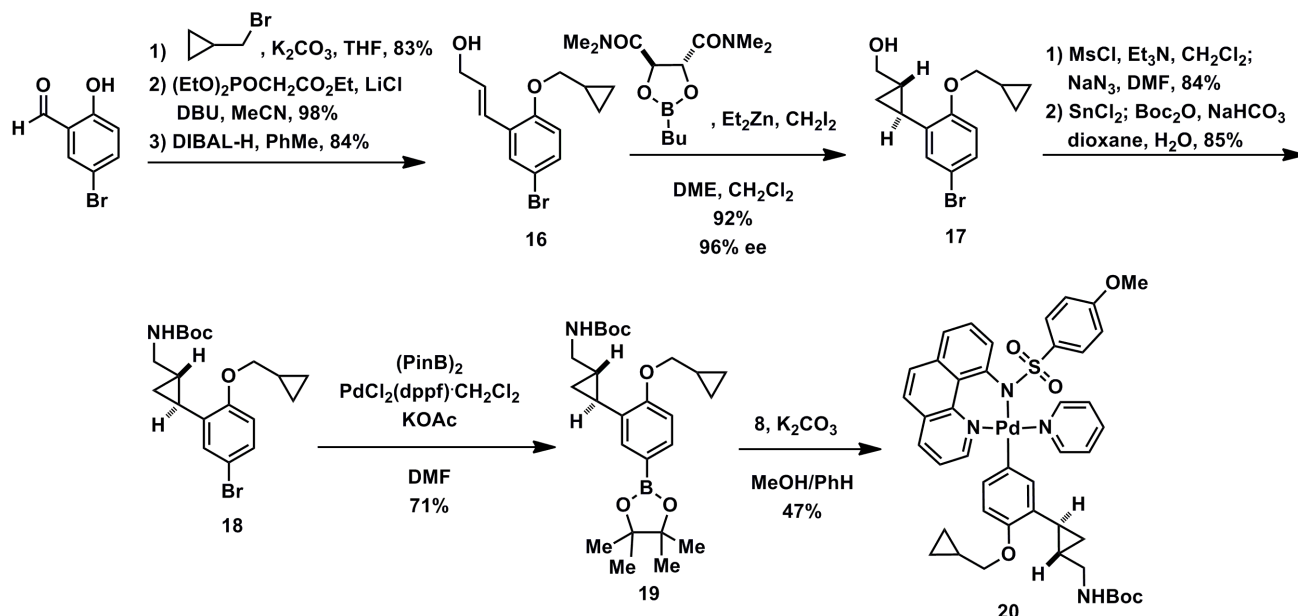


**Figure 6. Synthesis of palladium(II) aryl substrate 20.**

doi:10.1371/journal.pone.0059187.g006



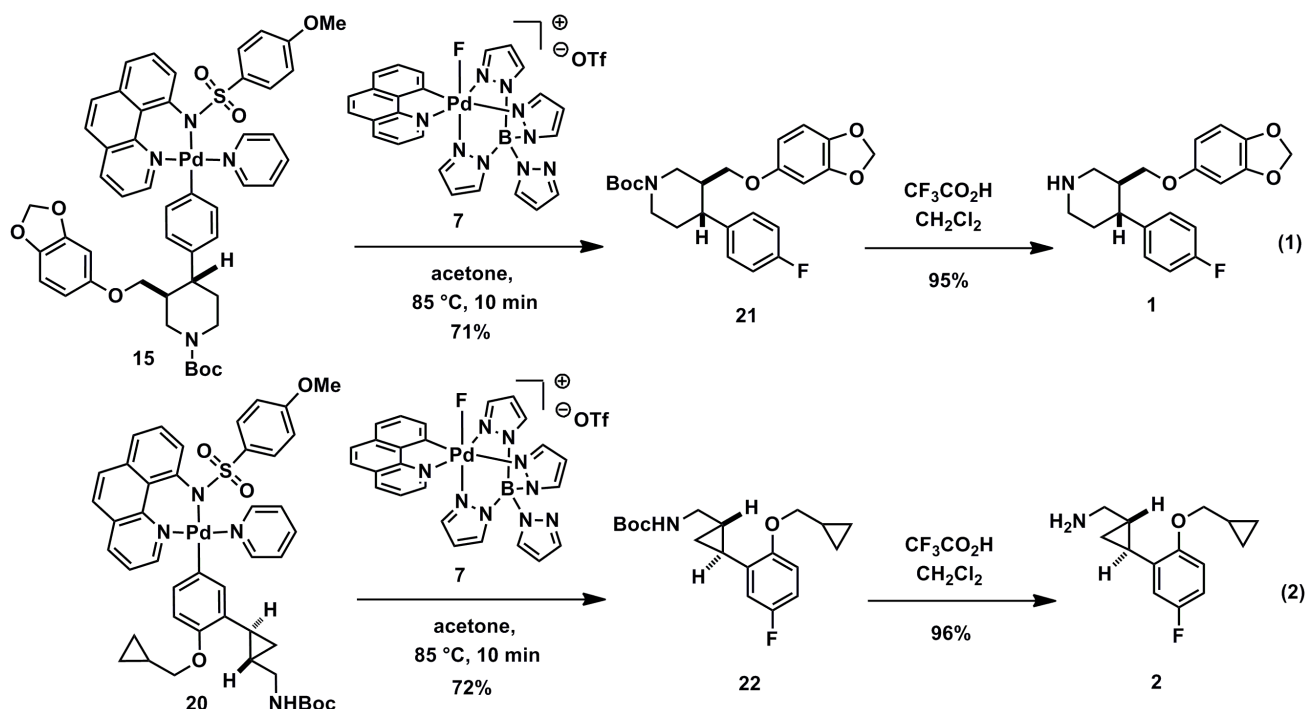


**Figure 7. Synthesis of aryl fluorides 1 and 2 via late-stage fluorination with electrophilic reagent 7.**  
doi:10.1371/journal.pone.0059187.g007

the picoline ligand. After filtration, the palladium aryl substrate is added, and the resulting solution was heated at 85°C in a sealed vial.

Generally, radiochemistry methods are first explored using hand manipulations on a small amount of radioactivity (<500  $\mu\text{Ci}$  of [ $^{18}\text{F}$ ]fluoride). However, a typical PET imaging experiment in NHPs requires 5–10 mCi of final radiolabeled pure product, which along with the efficiency of the reaction dictates that the starting amount of [ $^{18}\text{F}$ ]fluoride needs to be anywhere from 50 mCi to 1 Ci of radioactivity. Currently, our fluorination method requires starting with 1 Ci to produce enough for NHP PET imaging experiments. Due to safety considerations, automated synthesis protocols were developed using a commercially-available platform and took place inside of a hot cell. Synthesis modules were programmed to run the reaction (azeotropic drying, fluoride capture, filtration, and fluorination; see Supporting Information S1). The automated procedures can now be used to produce tens of mCi of radiolabeled aryl fluorides prior to purification (Figure 8B and 3C).

Post synthesis protocols include 1) filtration through a plug of silica to remove bulk metal contaminants, 2) removal of protecting groups, 3) HPLC purification for isolation, and 4) formulation in a sterile solution for administration. Post synthesis manipulations are currently conducted by hand, though ideally will be automated in the future.

While protecting groups are common in radiochemistry, deprotection reactions must be fast and efficient. For the two radiolabeled molecules in this research, we chose to protect the primary and secondary amines with easily removable *t*-butoxycarbonyl (Boc) groups. Exposure of [ $^{18}\text{F}$ ]-21 and [ $^{18}\text{F}$ ]-22 to trifluoroacetic acid for two minutes revealed the ammonium salts.

Because the mass of fluorinated material using high specific activity [ $^{18}\text{F}$ ]fluoride is typically less than 10  $\mu\text{g}$  among milligrams of reaction reagents, HPLC can be an efficient and often used [35]

tool to remove contaminants and byproducts. We have devised routine HPLC methods that purify [ $^{18}\text{F}$ ]-1 and [ $^{18}\text{F}$ ]-2 with standard semi-preparatory columns in less than 15 minutes. Final samples are chemically and radiochemically pure and have less than 5 parts per billion palladium (ppb) content, well below suggested guidelines for use in humans (<1000 ppb) [36]. The residual amount of palladium was determined by inductively coupled plasma mass spectroscopy (ICP-MS) analysis.

After HPLC purification, the sample is captured with a solid phase extraction column and formulated in a sterile saline solution. Final samples were analyzed for purity, residual solvent, pH, pyrogenicity, and sterility and passed all quality control protocols generally used for PET imaging in NHPs.

Starting with an approximated 1 Ci of radioactivity, our method can be used to produce >10 mCi of formulated product in up to 13 Ci/ $\mu\text{mol}$  specific activity at time of injection (TOI), suitable for imaging primates. *The entire process from obtaining aqueous samples of  $^{18}\text{F}$  through formulation can be accomplished in less than 100 min.*

#### Non-human Primate PET Imaging with [ $^{18}\text{F}$ ]-1 and [ $^{18}\text{F}$ ]-2

Using the procedure outlined above, we prepared [ $^{18}\text{F}$ ]-1 and [ $^{18}\text{F}$ ]-2 for use in four separate MR-PET imaging experiments in baboons (*Papio anubis*). The objective of these studies was to determine the brain pharmacokinetic profile and distribution of [ $^{18}\text{F}$ ]-1 and [ $^{18}\text{F}$ ]-2 and compare the binding and kinetic profile to scans performed after a drug challenge. This “test-block” procedure provides information about the nature of the radioactive signal that is observed. The initial protocol is designed to determine the contribution of specific and non-specific binding to the PET signal. Specific binding interactions, (i.e. [ $^{18}\text{F}$ ]-1 with SERT [37]; [ $^{18}\text{F}$ ]-2 with 5-HT<sub>2C</sub>), will undergo competition with drug pretreatment resulting in an overall reduced PET signal; however binding interactions that are non-specific and not in competition with the drug will remain the same. Determining the

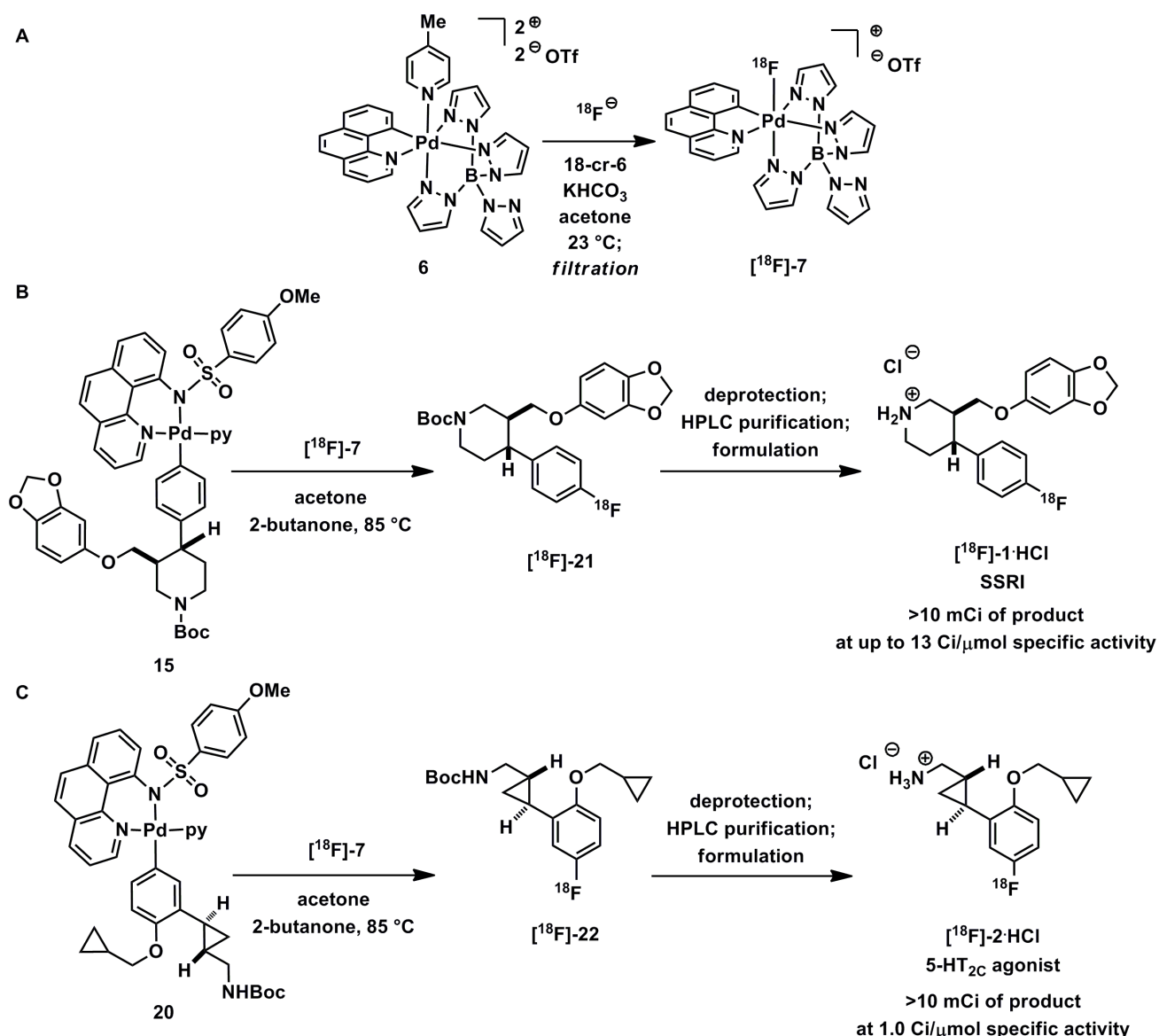


**Figure 8. Palladium-mediated synthesis of [<sup>18</sup>F]-1 and [<sup>18</sup>F]-2 using [<sup>18</sup>F]-7 derived from [<sup>18</sup>F]fluoride.** (A) Synthesis of the electrophilic fluorination reagent [<sup>18</sup>F]-7 for reaction with palladium aryl complexes. (B) Synthesis of SSRI [<sup>18</sup>F]-1 on a scale suitable for NHP PET imaging. (C) Synthesis of 5-HT<sub>2C</sub> agonist [<sup>18</sup>F]-2 on a scale suitable for NHP PET imaging.  
doi:10.1371/journal.pone.0059187.g008

extent to which the signal observed is a specific binding interaction is the first and most crucial step in radiotracer validation for receptor systems in the brain; it is also one of the least predictable outcomes in radiotracer development [38]. We chose blocking drugs (citalopram [39] 5.0 mg/kg for SERT; ritanserin [40] 0.1 mg/kg for 5-HT<sub>2C</sub>) that were known to be safe for administration intravenously [41,42] rather than performing self-saturation experiments with the non-radioactive analogs of [<sup>18</sup>F]-1 and [<sup>18</sup>F]-2.

Radiolabeling drug molecules with positron-emitting isotopes has intrinsic value, which is particularly true of central nervous system (CNS) drugs. Inferences about brain penetration and pharmacokinetic profile (PK) in humans are often made through extrapolation from studies in lower mammals and drug concentrations in human plasma, because observing drug concentration at target sites *in vivo* in humans is challenging.

Many drug molecules, commonly prescribed for the human CNS, are used without any knowledge of human brain PK. Understanding the brain distribution and kinetic profile of drugs or drug candidates in humans can help understanding drug failures and may ultimately provide better predictive tools for success in drug development [43,44]. While there are many reasons why drugs are not often labeled and evaluated with PET, a striking number of molecules cannot be labeled with either of the two most common PET isotopes, carbon-11 and fluorine-18. Paroxetine, a selective serotonin reuptake inhibitor, is a good example of a molecule that was previously considered inaccessible for high specific activity labeling approaches. The challenge of labeling paroxetine (**1**) was overcome using palladium-mediated fluorination and provided [<sup>18</sup>F]-1 in suitable yield for initial studies in NHPs.



## PET Study to Evaluate Biodistribution and Pharmacokinetic Profile

Two MR-PET imaging studies were performed with [<sup>18</sup>F]-**1**, a baseline and a challenge with citalopram, a competitive serotonin reuptake inhibitor. The baseline scan revealed modest brain penetration (0.013% ID/cc) corresponding to about 1.7% of the total injected dose accumulating in the brain. Penetration into and accumulation in the brain were rapid (Figure 9), reaching a plateau between 15–30 min. Washout kinetics were markedly slow with a  $t_{1/2}$  calculated from the data (35–90 min) of 21.3 h. This is consistent with the plasma half-life range (21–24 h) reported in the monograph for Paxil [45] (one of the trade-names for paroxetine). The accumulation of [<sup>18</sup>F]-**1** represents predominantly non-specific uptake in the brain. Heterogeneous binding was observed, but was inconsistent with the known SERT distribution from PET studies with validated radiotracers such as [<sup>11</sup>C]DASB [23]. The lack of specific binding was confirmed by citalopram challenge, in which there was no significant change in the accumulation and distribution of [<sup>18</sup>F]-**1** relative to baseline. Although data analysis with [<sup>18</sup>F]-**1** may be limited by the high degree of non-specific binding, the prevalence of paroxetine used to treat depression warrants evaluation of brain PK and distribution in humans.

## PET Study to Evaluate a Potential PET Radiotracer

Our choice to evaluate [<sup>18</sup>F]-**2** as a selective radiotracer for the serotonin 2c (5-HT<sub>2c</sub>) receptor was based upon the growing associations between 5-HT<sub>2c</sub> and brain-related disorders [46,47,48,49]. Although the associations exist, the 5-HT<sub>2c</sub> receptor has previously received less attention in psychopharmacology and neuroimaging than its homolog, 5-HT<sub>2A</sub>. To date, selective 5-HT<sub>2c</sub> radioligands for autoradiography and 5-HT<sub>2c</sub> radiotracers for imaging have not been described, a fact which has no doubt hindered research in neurobiology. Due to the recent development of novel scaffolds for potent and selective ligands of 5-HT<sub>2c</sub>, *in vivo* imaging of 5-HT<sub>2c</sub> has become a realistic goal [46]. Very few, if any, of the molecules that selectively target 5-HT<sub>2c</sub> are obvious labeling candidates for either carbon-11 or fluorine-18; much less, compounds for which *in vivo* data support the likelihood for radiotracer development success. Agonist **2** was chosen from the literature not only because it was well-suited for the chemistry described, but also because of its selectivity profile (40-fold and 14-fold selective for 5-HT<sub>2c</sub> over 5-HT<sub>2A</sub> and 5-HT<sub>2B</sub>, respectively) and its demonstrated efficacy in an animal model of antipsychotic drug activity [21]. To our knowledge, this

is the first reported evaluation of a 5-HT<sub>2c</sub>-targeted molecule for use in PET.

Two preliminary imaging studies in non-human primates were used to determine whether [<sup>18</sup>F]-**2** exhibited suitable blood-brain penetration, pharmacokinetic profile, and specific binding suitable for use as a 5-HT<sub>2c</sub> PET tracer (Figure 10). Data from the baseline study indicate that [<sup>18</sup>F]-**2** has excellent brain penetration with an average brain : plasma ratio of 1.5 at 30 minutes post injection. Analysis of arterial plasma from this experiment suggested that the compound had suitable metabolic stability (nearly 70% of radioactivity in plasma was associated with intact [<sup>18</sup>F]-**2** at 60 min) to warrant continuation to pharmacological challenge studies. For the initial drug challenge, we chose ritanserin, which is a non-selective 5-HT<sub>2A</sub> (EC<sub>50</sub> = 4.6 nM), 5-HT<sub>2B</sub> (2.2 nM), and 5-HT<sub>2c</sub> (6.6 nM) antagonist [50]. We observed a modest 15% decrease in uptake of [<sup>18</sup>F]-**2** following ritanserin administration. The decrease was observed in the thalamus and throughout the cortex (frontal, medial parietal and temporal), but not in the cerebellum. Decreases in the thalamus and cortex are reasonably correlated with expectations from 5-HT<sub>2c</sub> mRNA mapping in the monkey [51] and human brains [52] *ex vivo*. The lack of blockade in the cerebellum is also consistent with the assumed 5HT<sub>2c</sub> receptor distribution. One notable exception is that higher levels of uptake and blockade were anticipated in the choroid plexus. Our preliminary data, which indicate modest specific binding, are encouraging and warrant additional studies to more accurately quantify the reduction in binding potential of [<sup>18</sup>F]-**2** during pharmacological challenge.

## Methods

See Supporting Information S1.

## Conclusions

We have developed a modern fluorination reaction with large substrate scope that can be used for the synthesis of complex <sup>18</sup>F-labeled aryl fluorides suitable for imaging in NHPs. Our synthesis of radiolabeled aryl fluorides employs [<sup>18</sup>F]fluoride, is fast, high-yielding, and affords only one aryl fluoride constitutional isomers and no inseparable byproducts. We have demonstrated that our method can be translated to synthesize radiolabeled aryl fluorides [<sup>18</sup>F]-**1** and [<sup>18</sup>F]-**2** in quantity and quality suitable for PET imaging studies in baboons to obtain pharmacokinetic data. Our method can tolerate a large variety of functional groups, and is suitable for electron-rich and -deficient arenes, which is a

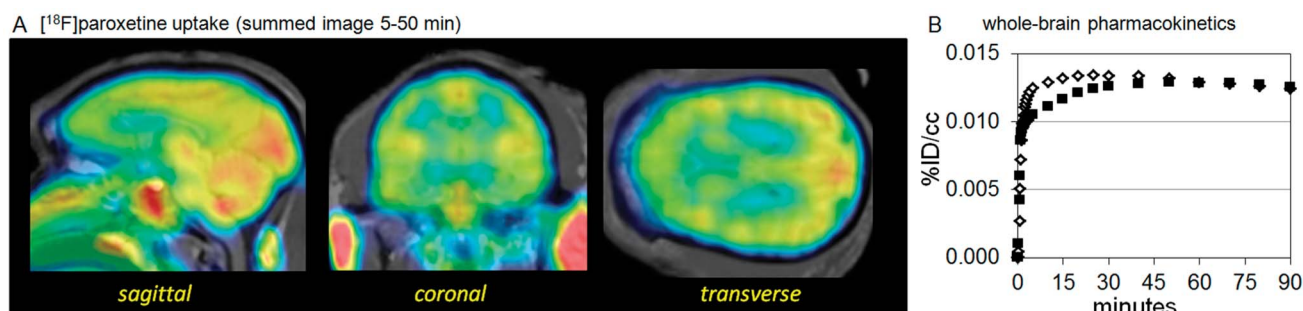


**Figure 9. Distribution and pharmacokinetic profile of [<sup>18</sup>F]paroxetine ([<sup>18</sup>F]-**1**) from MR-PET imaging in non-human primates.** (A) Summed images from 5–50 min of the dynamic PET collected following injection of [<sup>18</sup>F]-**1**. The images are fused with a structural (T1 weighted) MR image. Although [<sup>18</sup>F]-**1** is a potent and selective ligand for the serotonin transporter (SERT), the observed binding does not match the distribution of SERT. This is indicative of high non-specific binding. The images highlight the overall high blood-brain-barrier penetration of [<sup>18</sup>F]-**1** and heterogeneity of binding observed. (B) Whole-brain average time-activity curves from [<sup>18</sup>F]-**1** from baseline and pretreatment (citalopram) studies. doi:10.1371/journal.pone.0059187.g009

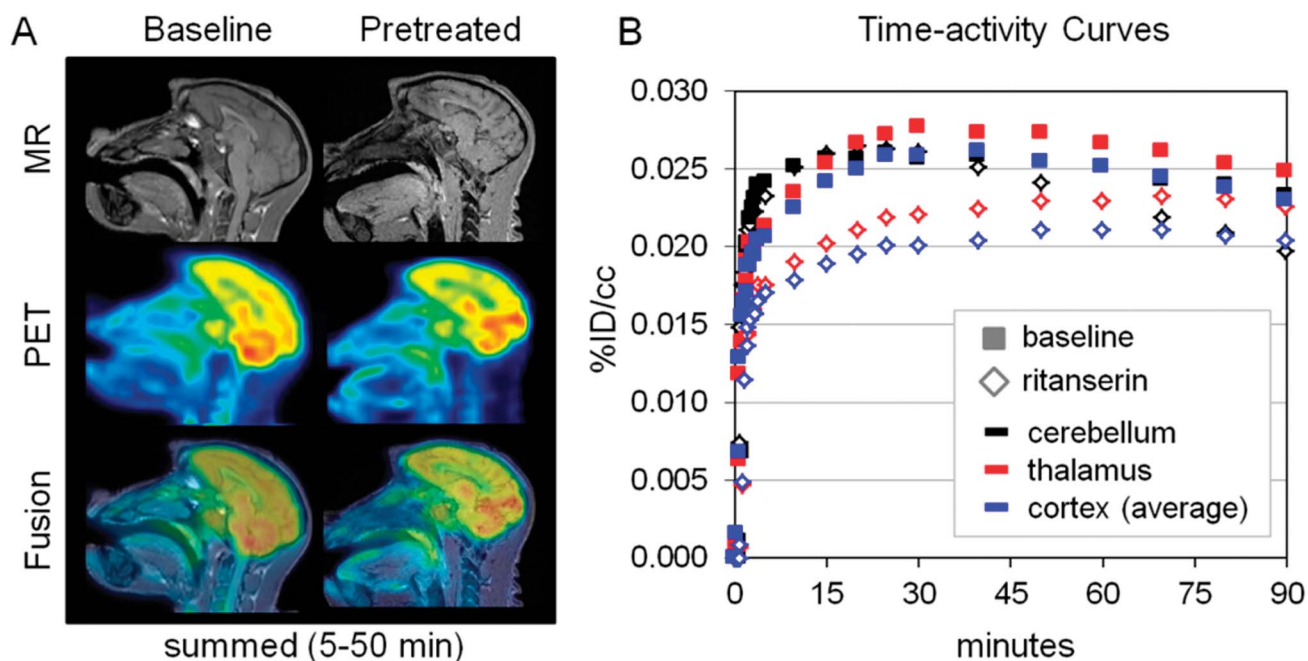


**Figure 10. Preliminary [<sup>18</sup>F]-2 MR-PET imaging in non-human primates.** (A) Summed images from 5–50 min of the dynamic PET collected following two studies (baseline and ritanserin pretreated) with [<sup>18</sup>F]-2. The images highlight the overall high blood-brain-barrier penetration of [<sup>18</sup>F]-2 and heterogeneity of binding observed. The highest concentrations were noted in the thalamus, cerebellum, and occipital cortex. (B) Time-activity curves from region-of-interest (ROI) analysis from the dynamic data represented in A. As seen in the kinetic profiles, ritanserin did not fully block the uptake of [<sup>18</sup>F]-2; however it did reduce binding and alter the pharmacokinetic profile in the thalamus and cortex but not the cerebellum. The extent to which this represents 5HT<sub>2c</sub> binding will require validation by additional imaging experiments.  
doi:10.1371/journal.pone.0059187.g010

challenge for conventional fluorination reactions. Current limitations of the method are the inability to tolerate certain nucleophilic functional groups, most notably tertiary amines, and the substantially lower yields for substrates with ortho substitution. Moreover, our method is not as simple to perform as a conventional nucleophilic aromatic substitution reaction and requires the synthesis of organotransition metal reagents.

We see utility in our method for the predictable synthesis of <sup>18</sup>F-labeled molecules that can support drug development, for example, small molecule drug candidates with drug-like structures such as paroxetine can now be labeled. In addition, we provide a tool that enables the synthesis of <sup>18</sup>F-labeled molecules for evaluation as potential PET tracers that report on a biological function. PET tracer development is challenging beyond synthesis, as exemplified by the high-nonspecific binding of paroxetine, which makes [<sup>18</sup>F]paroxetine ([<sup>18</sup>F]-1) unsuitable for imaging of SERT. But the ability to make more complex and structurally more diverse <sup>18</sup>F-labeled molecules more quickly, more reliably, and more efficiently than previously possible, may shift the future challenge toward PET tracer development rather than PET tracer synthesis. New fluorination methods that expand the number and types of molecules that can be radiolabeled blended with advances in tracer development should increase the impact of PET imaging.

## References

1. Fowler JS, Wolf AP (1997) Working against Time: Rapid Radiotracer Synthesis and Imaging the Human Brain. *Acc Chem Res* 30: 181–188.
2. Phelps ME (2000) Positron emission tomography provides molecular imaging of biological processes. *P Natl Acad Sci USA* 97: 9226–9233.
3. Miller PW, Long NJ, Vilar R, Gee AD (2008) Synthesis of C-11, F-18, O-15, and N-13 Radiolabels for Positron Emission Tomography. *Angew Chem, Int Ed* 47: 8998–9033.
4. Ametamey SM, Honer M, Schubiger PA (2008) Molecular imaging with PET. *Chem Rev* 108: 1501–1516.
5. Muller K, Fach C, Diederich F (2007) Fluorine in pharmaceuticals: Looking beyond intuition. *Science* 317: 1881–1886.
6. Purser S, Moore PR, Swallow S, Gouverneur V (2008) Fluorine in medicinal chemistry. *Chem Soc Rev* 37: 320–330.
7. Cai LS, Lu SY, Pike VW (2008) Chemistry with [F-18]fluoride ion. *Eur J Org Chem*: 2853–2873.

In this respect, we are particularly excited about a new method developed in our group, which is based on nickel complexes [53], and may be more easily executed, also by the non-expert.

## Supporting Information

**Supporting Information S1 Contains details on materials and methods, experimental data for chemistry and radiochemistry, and spectroscopic data.**  
(PDF)

## Acknowledgments

We thank Helen Deng, Grae Arabasz, Shirley Hsu, and Joe Mandeville (Massachusetts General Hospital) for assistance with non-human primate PET imaging experiments. We thank the Caravan Lab (Harvard Medical School and Massachusetts General Hospital) for ICP-MS analysis.

## Author Contributions

Conceived and designed the experiments: ASK CNN JMH TR. Performed the experiments: ASK CNN EL SMC CKM NS. Analyzed the data: ASK CNN JMH TR. Contributed reagents/materials/analysis tools: EL SMC CKM NS. Wrote the paper: ASK JMH TR.

8. Furuya T, Kuttruff CA, Ritter T (2008) Carbon-fluorine bond formation. *Curr Opin Drug Discov Devel* 11: 803–819.
9. Furuya T, Kamlet AS, Ritter T (2011) Catalysis for fluorination and trifluoromethylation. *Nature* 473: 470–477.
10. O'Hagan D (2008) Understanding organofluorine chemistry. An introduction to the C-F bond. *Chem Soc Rev* 37: 308–319.
11. Bergman J, Solin O (1997) Fluorine-18-labeled fluorine gas for synthesis of tracer molecules. *Nucl Med Biol* 24: 677–683.
12. Emsley J (1980) Very Strong Hydrogen-Bonding. *Chem Soc Rev* 9: 91–124.
13. Hummer G, Pratt LR, Garcia AE (1996) Free energy of ionic hydration. *J Phys Chem* 100: 1206–1215.
14. Cabarcos OM, Weinheimer CJ, Lisy JM, Xantheas SS (1999) Microscopic hydration of the fluoride anion. *J Chem Phys* 110: 5–8.
15. Serdons K, Verbruggen A, Bormans GM (2009) Developing new molecular imaging probes for PET. *Methods* 48: 104–111.
16. Serdons K, Terwinghe C, Van Vermaelen P, Laere K, Kung H, et al. (2009) Synthesis and Evaluation of 18F-Labeled 2-Phenylbenzothiazoles as Positron Emission Tomography Imaging Agents for Amyloid Plaques in Alzheimer's Disease. *J Med Chem* 52: 1428–1437.
17. Antoni G, Langstrom B (2008) Radiopharmaceuticals: molecular imaging using positron emission tomography. *Handb Exp Pharmacol*: 177–201.
18. Modern Medicine website. Available: <http://drugtopics.modernmedicine.com/drugtopics/data/articlestandard//drugtopics/252011/727243/article.pdf>. Accessed 2013 Feb 14.
19. Landvatter SW, Ganes KT, Dannals RF (1998) Progress in the synthesis of paroxetine-[18F]. In: Heys JR, Melillo DG, editors. *Synthesis and Applications of Isotopically Labeled Compounds* 1997. England: John Wiley & Sons Ltd. 99–102.
20. Suehiro M, Wilson AA, Scheffel U, Dannals RF, Ravert HT, et al. (1991) Radiosynthesis and Evaluation of N-(3-F-18 fluoropropyl)paroxetine as a Radiotracer for In Vivo Labeling of Serotonin Uptake Sites by PET. *Nucl Med Biol* 18: 791–796.
21. Kozikowski AP, Cho SJ, Jensen NH, Allen JA, Svennebring AM, et al. (2010) HTS and Rational Drug Design to Generate a Class of 5-HT<sub>2C</sub>-Selective Ligands for Possible Use in Schizophrenia. *ChemMedChem* 5: 1221–1225.
22. O'Neil PM, Smith SR, Weissman NJ, Fidler MC, Sanchez M, et al. (2012) Randomized Placebo-Controlled Clinical Trial of Lorcaserin for Weight Loss in Type 2 Diabetes Mellitus: The BLOOM-DM Study. *Obesity* 20: 1426–1436.
23. Saulin A, Savli M, Lanzenberger R (2012) Serotonin and molecular neuroimaging in humans using PET. *Amino Acids* 42: 2039–2057.
24. Lee E, Kamlet AS, Powers DC, Neumann CN, Boursalian GB, et al. (2011) A Fluoride-Derived Electrophilic Late-Stage Fluorination Reagent for PET Imaging. *Science* 334: 639–642.
25. Teare H, Robins EG, Arstad E, Sajinder KL, Gouverneur V (2007) Synthesis and reactivity of [F-18]-N-fluorobenzenesulfonimide. *Chem Comm*: 2330–2332.
26. Teare H, Robins EG, Kirjavainen A, Forsback S, Sandford G, et al. (2010) Radiosynthesis and Evaluation of (18F)F Selectfluor bis(triflate). *Angew Chem, Int Ed* 49: 6821–6824.
27. Fowler JS, Shiue CY, Wolf AP, Salvadori PA, Macgregor RR (1982) Synthesis of F-18-labeled acetyl hypofluorite for radiotracer synthesis. *J Labelled Compd Radiopharm* 19: 1634–1636.
28. Furuya T, Ritter T (2008) Carbon-fluorine reductive elimination from a high-valent palladium fluoride. *J Am Chem Soc* 130: 10060–10061.
29. Furuya T, Benitez D, Tkatchouk E, Strom AE, Tang PP, et al. (2010) Mechanism of C-F Reductive Elimination from Palladium(IV) Fluorides. *J Am Chem Soc* 132: 3793–3807.
30. Furuya T, Kaiser HM, Ritter T (2008) Palladium-mediated fluorination of arylboronic acids. *Angew Chem, Int Ed* 47: 5993–5996.
31. Luedtke AT, Goldberg KI (2007) Reductive elimination of ethane from five-coordinate platinum(IV) alkyl complexes. *Inorg Chem* 46: 8496–8498.
32. Hughes G, Kimura M, Buchwald SL (2003) Catalytic enantioselective conjugate reduction of lactones and lactams. *J Am Chem Soc* 125: 11253–11258.
33. Charette AB, Juteau H, Lebel H, Molinaro C (1998) Enantioselective cyclopropanation of allylic alcohols with dioxaborolane ligands: Scope and synthetic applications. *J Am Chem Soc* 120: 11943–11952.
34. Cai L, Lu S, Pike VW (2008) Chemistry with [18F]Fluoride Ion. *Eur J Org Chem* 2008: 2853–2873.
35. Shao X, Hoareau R, Hockley BG, Tluczek IJM, Henderson BD, et al. (2011) Highlighting the versatility of the tracerlab synthesis modules. Part 1: fully automated production of F-18 labelled radiopharmaceuticals using a Tracerlab FXFN. *J Labelled Compd Radiopharm* 54: 292–307.
36. European Medicines Agency website. Available: [www.ema.europa.eu/docs/en\\_GB/document\\_library/Scientific\\_guideline/2009/09/WC500003587.pdf](http://www.ema.europa.eu/docs/en_GB/document_library/Scientific_guideline/2009/09/WC500003587.pdf). Accessed 2013 Feb 14.
37. Owens MJ, Morgan WN, Plott SJ, Nemeroff CB (1997) Neurotransmitter Receptor and Transporter Binding Profile of Antidepressants and Their Metabolites. *J Pharmacol Exp Ther* 283: 1305–1322.
38. Jiang ZJ, Reilly J, Everatt B, Briard E (2011) A rapid vesicle electrokinetic chromatography method for the in vitro prediction of non-specific binding for potential PET ligands. *J Pharmaceut Biomed* 54: 722–729.
39. Hinz R, Selvaraj S, Murthy NV, Bhagwagar Z, Taylor M, et al. (2008) Effects of citalopram infusion on the serotonin transporter binding of C-11 DASB in healthy controls. *J Cerebr Blood F Met* 28: 1478–1490.
40. Coenen HH, Wienhard K, Stocklin G, Laufer P, Hebold I, et al. (1988) PET Measurement of D<sub>2</sub> and S<sub>2</sub> Receptor-Binding of 3-N(2'-F-18 fluoroethyl)spiperone in Baboon Brain. *Eur J Nucl Med* 14: 80–87.
41. Pinborg LH, Feng L, Haahr ME, Gillings N, Dyssegaard A, et al. (2012) No change in [11C]CUMI-101 binding to 5-HT<sub>1A</sub> receptors after intravenous citalopram in human. *Synapse (New York)* 66: 880–884.
42. Centurion D, Sanchez-Lopez A, Ortiz MI, De Vries P, Saxena PR, et al. (2000) Mediation of 5-HT-induced internal carotid vasodilatation in GR127935- and ritanserin-pretreated dogs by 5-HT<sub>7</sub> receptors. *N-S Arch Pharmacol* 362: 169–176.
43. Bergstrom M, Grahnen A, Langstrom B (2003) Positron emission tomography microdosing: a new concept with application in tracer and early clinical drug development. *Eur J Clin Pharmacol* 59: 357–366.
44. Wang JL, Maurer L (2005) Positron emission tomography: Applications in drug discovery and drug development. *Curr Top Med Chem* 5: 1053–1075.
45. GlaxoSmithKline website. Available: [http://www.gsk.ca/english/docs-pdf/Paxil\\_2011.pdf](http://www.gsk.ca/english/docs-pdf/Paxil_2011.pdf). Accessed 2013 Feb 14.
46. Monck NJ, Kennett GA (2008) 5-HT<sub>2C</sub> ligands: recent progress. *Prog Med Chem* 46: 281–390.
47. Christianson JP, Ragole T, Amat J, Greenwood BN, Strong PV, et al. (2010) 5-Hydroxytryptamine 2C Receptors in the Basolateral Amygdala Are Involved in the Expression of Anxiety After Uncontrollable Traumatic Stress. *Biol Psychiat* 67: 339–345.
48. Siuciak JA, Chapin DS, McCarthy SA, Guanowsky V, Brown J, et al. (2007) CP-809,101, a selective 5-HT<sub>2C</sub> agonist, shows activity in animal models of antipsychotic activity. *Neuropharmacology* 52: 279–290.
49. Pandey SC, Lumeng L, Li TK (1996) Serotonin(2C) receptors and serotonin(2C) receptor-mediated phosphoinositide hydrolysis in the brain of alcohol-preferring and alcohol-nonpreferring rats. *Alcohol Clin Exp Res* 20: 1038–1042.
50. Knight AR, Misra A, Quirk K, Benwell K, Revell D, et al. (2004) Pharmacological characterisation of the agonist radioligand binding site of 5-HT<sub>2A</sub>, 5-HT<sub>2B</sub> and 5-HT<sub>2C</sub> receptors. *N-S Arch Pharmacol* 370: 114–123.
51. Lopez-Gimenez JF, Mengod G, Palacios JM, Vilario MT (2001) Regional distribution and cellular localization of 5-HT<sub>2C</sub> receptor mRNA in monkey brain: Comparison with H-3 mesulergine binding sites and choline acetyltransferase mRNA. *Synapse (New York)* 42: 12–26.
52. Pasqualetti M, Ori M, Castagna M, Marazziti D, Cassano GB, et al. (1999) Distribution and cellular localization of the serotonin type 2C receptor messenger RNA in human brain. *Neuroscience* 92: 601–611.
53. Lee E, Hooker JM, Ritter T (2012) Nickel-Mediated Oxidative Fluorination for PET with Aqueous F-18 Fluoride. *J Am Chem Soc* 134: 17456–17458.